Research Article Vol. 30, No. 12 / 6 Jun 2022 / Optics Express 21468

Optics EXPRESS

Controllable high-speed rotated femtosecond cylindrical vector beam based on optical heterodyne interference

YUWEI ZHAO,[1] JINTAO FAN,[1,2] YOUJIAN SONG,[1] AND MINGLIE HU[1,3]

[1] *Ultrafast Laser Laboratory, Key Laboratory of Opto-electronic Information Science and Technology of Ministry of Education, School of Precision Instruments and Opto-electronics Engineering, Tianjin University, 300072 Tianjin, China*
[2] *fanjintao@tju.edu.cn*
[3] *huminglie@tju.edu.cn*

Abstract: Structured light beams that possess unique polarization distribution could offer a new degree of freedom for a variety of applications, and hence its flexible polarization manipulation is necessary. Here we experimentally report a heterodyne interference-based method for generating femtosecond cylindrical vector beam (CVB) with high-speed controllable rotated polarization states. The femtosecond CVBs are created through the superposition of two optical vortices with opposite handedness. The use of two acoustic-optical modulators (AOMs) with frequency differences allows to achieve polarization rotation in a hopping-free scheme at on demand speed. Up to 1 MHz of the rotation frequency is demonstrated by visualizing the fast rotation events through a fast-frame-rate CCD camera. Moreover, we show our method can be readily extended to produce higher order CVBs with more complex rotated polarization distributions. Such a simple yet versatile femtosecond polarization-controlled laser system has the capability to act as a nonlinear trapping platform, thus opening tremendous potential opportunities in the fields of micromachining, nanofabrication, and so force.

1. Introduction

Like amplitude, wavelength and phase, the polarization is one of the fundamental properties of light. Recently, there has been a growing interest in light beams with spatially variant polarization structures. Among them, cylindrical vector beam (CVB), acting as vector beam solution of the Maxwell's equation, features a cylindrically symmetry in polarization with a doughnut-shaped spatial intensity [1]. In general, radially and azimuthally polarized beams are the two most relevant examples of CVBs. Under tight focusing conditions, radial polarization yields a sharper focal spot, while azimuthal polarization can be focused into a hollow spot. Taking advantages of these unique properties, CVBs have exhibited potential applications in optical tweezers [2–4], electron acceleration [5], super-resolution microscopic imaging [6], optical communications [7–9] and to name a few. These exponentially growing application demands have triggered the development of various CVB sources. A typical method is to convert spatial homogeneous polarized Gaussian beam into CVB utilizing phase elements, including q-plates, space-variant subwavelength gratings, spatial light modulators (SLM), and others [10–12]. Alternatively, the methods for obtaining the CVBs directly at source have also been carried out, i.e., the annular beam as pump, the use of vortex retarder or mode-selective coupler (MSC) inside cavity [13–15]. In addition, nonlinear conversion techniques based on second harmonic generation [16] and optical parametric oscillators [17] have also been demonstrated to expand the available wavelength range of the CVBs. However, these techniques mainly focus on the generation of CVBs.

#460710 https://doi.org/10.1364/OE.460710
Journal © 2022 Received 8 Apr 2022; revised 23 May 2022; accepted 23 May 2022; published 31 May 2022

Optics EXPRESS

Indeed, to fully exploit the additional degree of freedom offered by CVBs for applications like optical trapping, it's essential to further develop novel systems that can rapidly control the polarization states of such beams. Within the field of optical trapping, one particularly important example is the rotation manipulation of small objects, which has been widely used in applications such as photo-mechanics, micro-machinery, micro-chemistry [18]. Using CVBs for rotation needs to make use of the change in polarization state of light upon propagation [19]. Among the possible strategies, the simplest way is to rotate half wave plate mechanically to adjust the polarization plane of the beam, so that the torque induced by the misalignment between the linearly polarized laser field and optical axis of the trapped particle is changed. This scheme, however, has two disadvantages: the rotation speed is limited and also hard to control. In principle, CVBs can be created by superposition of two circular polarized vortices with opposite OAM charges. Changing the phase difference is proven to be a valid approach to generate rotational polarized CVBs. By means of electro-optic modulators (EOMs) or photo-elastic modulators (PEMs), quasi-continuous rotation is realized limited by its wrapped phase modulation [20–22]. Very recently, applying a linear polarization synthesis scheme, Wei et. al presented a continuously rotation control system based on optical heterodyne interference in the continuous wave (CW) time scale [23]. Despite the CW trappings have already shown tremendously successful, femtosecond laser with high peak power and short pulse duration could stimulate nonlinear optical effects within the process of trapping particles, which is termed as nonlinear trapping, could satisfy more widespread applications [24]. Therefore, it is significant to create a compact device to create CVBs with a controllable hopping-free rotation rate in femtosecond time scale.

In this paper, we demonstrate a straightforward scheme to generate femtosecond CVBs, of which spatial phase and polarization distributions are in a controllable rotation fashion. The rotation is enabled by optical heterodyne interference between two optical vortices with opposite handedness. Two acoustic-optical modulators (AOMs) have been inserted into the interferometer to electronically adjust the rotation rate at arbitrary value. Femtosecond CVBs with rotation speed ranging from 1 kHz to 1 MHz are obtained. The rotation process can be witnessed by using a fast-frame-rate CCD camera. We further show that our scheme can be straightforwardly expanded to produce high order rotated CVBs by simply increasing the orders of vortex wave plates (VWP). The obtained results show the successful realization of high speed rotated femtosecond CVBs, which will extend the potential of nonlinear optical trapping.

2. Experimental setup

The experimental setup to generate and characterize high speed rotated femtosecond CVBs is schematically shown in Fig. 1. A home-built mode-locked Yb-doped fiber laser with a central wavelength around 1040 nm, repetition frequency of 53 MHz, and pulse duration of 105 fs is used as emitting source. The laser could deliver as much as 2 W average power in a linearly polarized beam with a Gaussian spatial profile. A telescope system composed of the lens1 (L1) and lens 2 (L2) with different focal lengths is used to determine the spot size of the incident beam, which should match aperture diameter of the AOMs. Herein, the focal lengths of lens L1 and L2 are chosen as 150 mm and 75 mm respectively, which ensures that the spot size is reduced to be a half of the original spot size (1.8 mm). Next, the beam is sent to the Mach–Zehnder interferometer (MZI) scheme, where the laser intensity is firstly divided by combination of a half-wave plate (HWP1) and a polarizing beam splitter (PBS1). Such a combination controls intensity distribution of each arm. Then, two copies of laser beams with orthogonally polarization states pass through different optical path and recombine at another polarizing beam splitter (PBS2). A pair of gold coated reflection mirrors is placed on a motorized translation stage serving as the time delay to finely tune the optical path differences, so that two copies of laser pulses could overlap well. Using the PBSs to split and combine the beam could improve the total output laser power [25].

Optics EXPRESS

After passing through a quarter waveplate (QWP) and a VWP, two orthogonal polarization beams would be converted into two optical vortices with opposite topological charges ($l_1 = 1$ and $l_2 = -1$) respectively. The superposition of these two optical vortices will lead to a CVB, which could be identified by a point-symmetric interference pattern after PBS3. Taking into account of the diffraction loss of the AOMs and the mode conversion loss of VWP, the created rotated CVBs has an average output power of about 1.73 W. A commercially available Charge Coupled Device (CCD) (Bobcat-320, Xenics) is employed to record a sequence of images for tracking the high-speed rotation events.

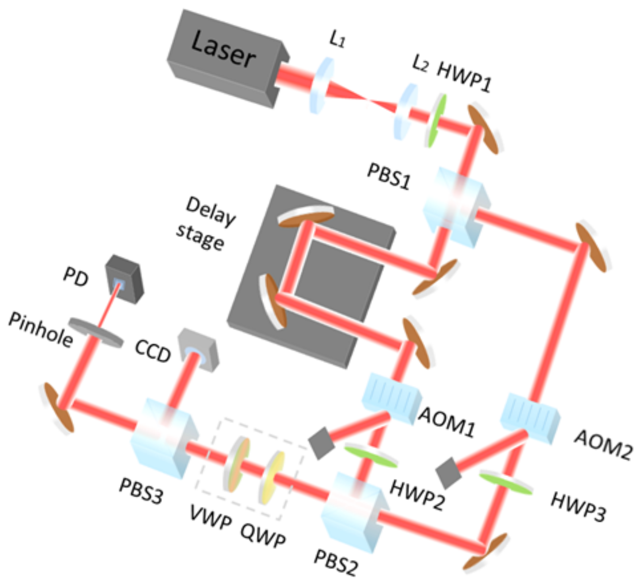

Fig. 1. Experimental setup. L, Lens; HWP, half-wave plate; PBS, polarization beam splitter; AOM, acoustic-optical modulator; QWP, quarter-wave plate; VWP, vortex wave-plate; PD, photodiode.

To obtain CVBs whose polarization states continuously change, it is required to have a time varying relative phase between two orthogonal polarized vortices. A valid method to realize a continuous phase shift in the time domain is to modulate the field in the frequency domain [26]. To this end, we introduce two AOMs in each MZI arm. The central operation frequency of the two acousto-optic crystals is 70 MHz with frequency stability of ± 1 Hz. Two RF (radio frequency) drive circuits with working frequency ranging from 70 MHz to 71 MHz with resolution of 50 Hz are used to drive the acousto-optic crystals. The two copies were frequency shifted to $f_0+\Delta f_1$ and $f_0+\Delta f_2$, respectively. f_0 is the central frequency of input beam, Δf_1 and Δf_2 are frequency shifts caused by the AOMs. Actually, we concentrate more on the heterodyne frequency Δf_1 - Δf_2, which will be directly translated into a linear phase shift in the time domain, thus determining the wanted rotation speed of CVBs. A photodiode (PD) is used to monitor the rotation frequency of the generated CVBs.

3. Working principle

The operation mechanism of the designed system is determined by the operation of the QWP, VWP, together with AOMs. The Jones matrix calculation is a well-known method for analyzing mode and polarization evolutions of light beams with complex polarization features [27–29].

Optics EXPRESS

Here, we provide a detailed discussion of the operation of proposed scheme, in terms of Jones matrices.

Considering the fact that the MZI is used to introduce time varying phase differences, to simplify the calculation, we firstly focus the polarization evolution after the two copies of pulses recombined after PBS2. Taking the Jones matrix of PBS into account, two orthogonally polarized beams are obtained for the right arm and left arm of the MZI, whose polarization states can be written as $\vec{E}_R=\frac{1}{\sqrt{2}}\begin{bmatrix}1\\0\end{bmatrix}$ and $\vec{E}_L=\frac{1}{\sqrt{2}}\begin{bmatrix}0\\1\end{bmatrix}$, respectively. After these two beams passing through a QWP with α=45°, the Jones vectors of the desired output beams are expressed as $\frac{1}{2}\begin{bmatrix}1\\-i\end{bmatrix}$ and $\frac{1}{2}\begin{bmatrix}1\\i\end{bmatrix}$. Clearly, right hand circularly polarized (RCP) and left hand circularly polarized (LCP) Gaussian beam are obtained here. In what follows, mode conversion process is realized by a VWP, which is a half-wave plate with an optic axis that varies as a function of the azimuthal angle. When operating on the orthogonally circular polarization states, the VWP produces $\frac{1}{2}e^{i\varphi}\begin{bmatrix}1\\-i\end{bmatrix}$ and $\frac{1}{2}e^{-i\varphi}\begin{bmatrix}1\\i\end{bmatrix}$, respectively. These two Jones vectors reveal the fact that optical vortices with left and right circular polarizations are generated in two different arms.

We then illustrate the influence of the AOMs inserted in MZI. In the proposed system, the laser frequencies in each arm are shifted to possess a slight difference, leading to a heterodyne interference arrangement. When a frequency shift Δf_1 is applied to the frequency domain, a linear phase shift $2\pi\Delta f_1$ will exists in the carrier phase of the light field while no effect on the polarization plane is occurred. Thus, by take the AOMs into account and at time t, the Jones vectors of the vortices can be expressed as: $\frac{1}{2}e^{i(2\pi\Delta f_1 t+\varphi_1)}\begin{bmatrix}1\\-i\end{bmatrix}$ and $\frac{1}{2}e^{-i(2\pi\Delta f_2 t+\varphi_2)}\begin{bmatrix}1\\i\end{bmatrix}$, respectively. The two vortices are recombined together. The resulting Jones Matrix can be depicted as:

$$\frac{1}{2}\left(e^{i(2\pi\Delta f_1 t+\varphi_1)}\begin{bmatrix}1\\-i\end{bmatrix}+e^{-i(2\pi\Delta f_2 t+\varphi_2)}\begin{bmatrix}1\\i\end{bmatrix}\right)=\begin{pmatrix}\cos(\pi\Delta f t+\varphi)\\\sin(\pi\Delta f t+\varphi)\end{pmatrix}, \tag{1}$$

where $\Delta f = \Delta f_2 - \Delta f_1$, and $\varphi = \varphi_2 - \varphi_1$. Δf_1 and Δf_2 represent the shifted frequency of the light field, respectively. Δf is the heterodyne frequency between two copies of light in MZI. φ is the initial phase difference of two copies introduced by the MZI. It should be notice that Eq. (1) indicates the CVB has a linear phase shift of $\pi\Delta f t$ resulting in a rotating polarization evolution over time, as illustrated in Fig. 2. In this way, arbitrary control of the rotational motion is achieved by the frequency difference between two AOMs [30]. In Fig. 2, we only show dynamic CVBs (including the radial, clockwise, azimuthal, anticlockwise polarization CVBs) and the corresponding interference pattern, at a time interval of $1/4\Delta f$. The modulated rotation is periodical at the angle of π, however, the accumulated phase is monotonously increasing, so that a hopping-free rotation is realized [23].

4. Experimental results

Given that CVBs generation process is sensitive to the phase difference between two optical vortices in each MZI arm, we need to carefully preset the optical length of the MZI. Assisted by an autocorrelator, a delicate overlap of two copies is realized. Then, to confirm the utility of the proposed method, we analyze the projected lobe structures after PBS3. Here, thanks to high resolution of the CCD, a two-fold symmetric lobe is clearly observed. This spatial structure further denotes the topological charge difference is 2, which is in good agreement with the optical vortex's order decided by the VWP.

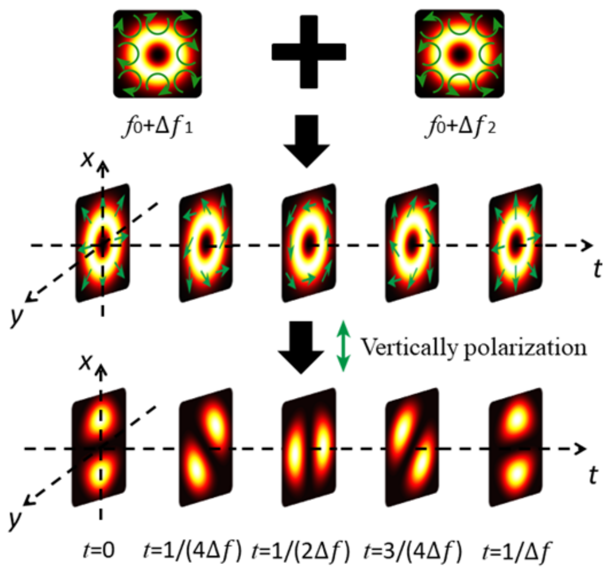

Fig. 2. Working principle of the generation of CVBs with a rotating polarization angle based on optical heterodyne interference. The CVBs are obtained by superposition of two optical vortices with topological charges $l_1 = 1$ and $l_2 = -1$, $\Delta f1$ and $\Delta f2$ are the frequency shifts caused by two AOMs respectively. Δf represents the heterodyne frequency of two laser beams.

Firstly, the working frequencies of AOM1 and AOM2 are set at 70 MHz and 70.001 MHz, respectively. To filter out the fundamental repetition rate of the laser, a low pass filter is used before we collected the rotated frequency of the lobes. Figure 3(a) presents the temporal signals of the generated lobes recorded by an oscilloscope. The period of signals shown in Fig. 3(a) is about 1 ms, which exactly corresponds to the heterodyne frequency between two arms. We also perform Fourier transform analysis on the recorded results of Fig. 3(a) to obtain its frequency distribution, as depicted in Fig. 3(b). The strongest frequency component is 1 kHz, which is the target rotation frequency we applied. Some harmonic signals are also found, this can be ascribed to the fact that the measured lobes have a two-fold rotational symmetry and the PD is positioned at only one lobe. Indeed, the linewidth of the frequency component can be effectively reduced by increasing the sampling points. A series of observation images of the created lobes at time interval of 0.25 ms (1/4 of the beating period) are shown in Fig. 3(c). The nonuniform occurring in the lobe patterns can be attributed to incomplete collimation of optical elements in our experiment and also a slight amount of astigmatism of the initial Gaussian beam. As expected, at 1 ms, 360 degrees of rotation of the first image is observed, reflecting the periodic rotation of the optical lobes, which indicates the validity of our method to generate high speed

Optics EXPRESS

rotated CVBs without mechanically moving parts. The continuously rotating dynamics of lobe patterns within 10 s can be found in supplementary Visualization 1.

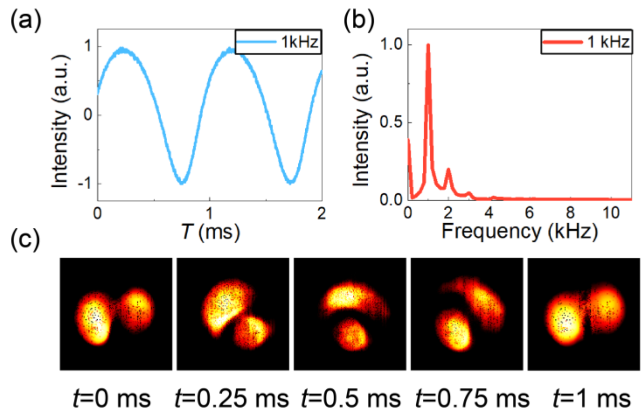

Fig. 3. The rotation dynamics of CVBs when the heterodyne frequency is set to 1 kHz. (a) The temporal signals of the rotated CVBs. (b) The frequency spectra obtained by Fourier transform to the signals in (a). (c) The interference patterns of the rotated CVBs captured by CCD.

Taking advantage of high controllability of the proposed method, it is possible to control the rotation movement at arbitrary speed. The heterodyne frequency can be easily tuned by means of setting the driving frequency of the AOM2, which will result in the angular velocity of the rotated lobes. As shown in Fig. 4(a) and Fig. 4(c), several rapid rotation movements are realized by setting the Δf between 2 kHz and 1 MHz. Notably, these rotations occur without any additional adjustments of any other components in our system, so that a simple rotation method is demonstrated. Fourier transforms are also performed, as displayed in Fig. 4(b) and Fig. 4(d). As can be seen from Fig. 4, the rotation frequencies agree well with the heterodyne frequencies. All the rotated motions of the lobe structure can be witnessed by CCD camera, as can be seen in supplementary Visualization 2, Visualization 3, Visualization 4, Visualization 5 and Visualization 6. Obviously, when the heterodyne frequency increases, the rotation of the movements becomes faster. It should be pointed out that our CCD is only able to distinguish the rotated lobes when the heterodyne frequency is below 70 kHz. However, we can still perceive the energy flows of the lobes by carefully watch the video. In principle, rotation control can be obtained in a wide frequency range from microhertz to megahertz, which is limited only by the working frequency of the AOMs. In addition, by changing the modulated frequency in AOMs, the sense of the rotation of the lobe structure can be readily controlled [19].

Figure 5 shows the recorded autocorrelation traces and pulse duration at the full width of half maximum (FWHM) from a second-harmonic intensity autocorrelator in dependence of heterodyne frequency. As can be seen from Fig. 5(a), the autocorrelation traces show a quite clean pulse, no further state pulses are observed over the scanning range of the autocorrelator from −25 to 25 ps. The pulse duration roughly stays constant to be 171 to 179 fs over the whole frequency tuning range. Assuming a hyperbolic secant pulse shape, the corresponding pulse duration is only around 110 fs. The quiet constant pulse width over the heterodyne frequency tuning range suggests the high stability of the system.

By changing the topological charge of the interfered vortices, it's possible to create more complex vector fields with controllable rotated polarization distribution. In the following, the heterodyne frequency is set to be 1 kHz again. Here, we show examples of generating CVBs with polarization orders 2 and 3, as shown in Fig. 6. The number of the symmetric optical lobes is determined by the topological charges of vortices. These lobes are rotated around the

Optics EXPRESS

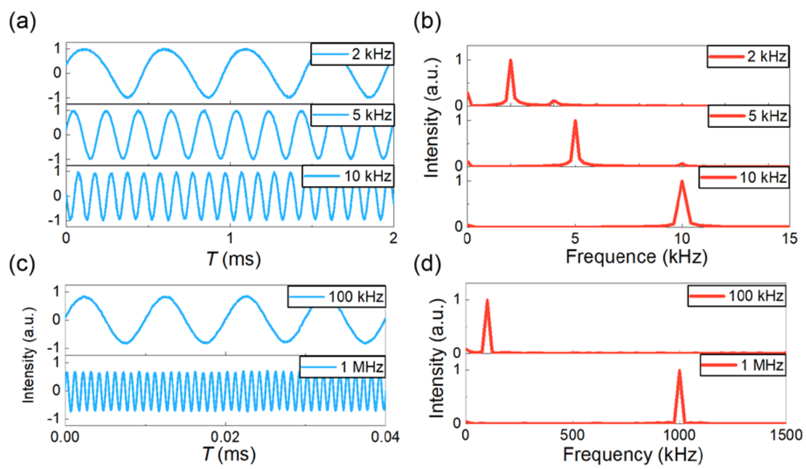

Fig. 4. (a), (c) Temporal signals of the rotated lobes at different heterodyne frequencies between 2 kHz and 1 MHz. (b), (d) The corresponding frequency spectra obtained by Fourier transform to the signals in (a), (c).

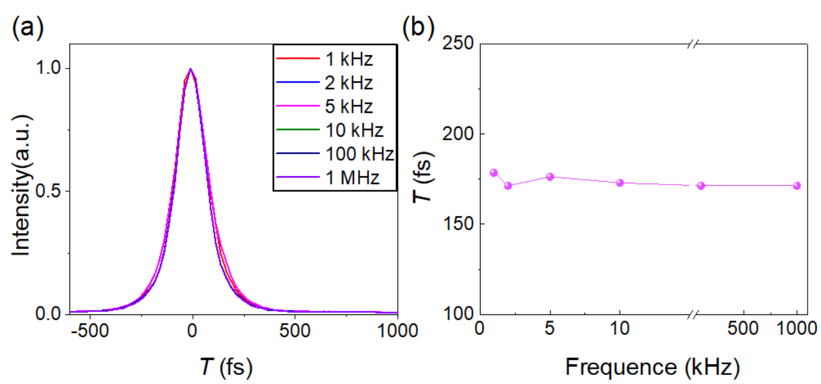

Fig. 5. (a) Autocorrelation traces when heterodyne frequency is set to be 1 kHz, 2 kHz, 5kHz, 10 kHz, 100 kHz and 1 MHz, respectively. (b) The calculated FWHM of autocorrelation traces in (a).

Optics EXPRESS

beam axis, here we present five images of the rotated lobes at time interval of 0.25 ms, which is equal to 1/4 of beat period. The corresponding video is recorded in the supplement materials (Visualization 7 and Visualization 8). Obviously, the polarization states are reproduced after one beat period, agreeing well with the designed heterodyne frequency. The time varying lobe shape remains nearly the same, indicating the highly polarized quality of the generated CVBs. In principle, the 1st and 2nd order CVB could serve as the basic unit to access the higher order CVBs, a $(j+k)^{th}$-order CVB can be readily generated after accumulating k groups of HWP and 1st order VWP after the jth-order CVB [31]. As a simple example, a 3rd order CVB is generated by inserting a HWP and a 1st order VWP after the 2nd order VWP. Notice that the rotation movement of the CVBs is freely controlled by the heterodyne frequency differences of two AOMs. Therefore, our technique can be readily extended to produce an arbitrary order CVBs with high speed rotated polarization structures, thus offering the ability of trapping and rotating different shaped objects and groups of objects.

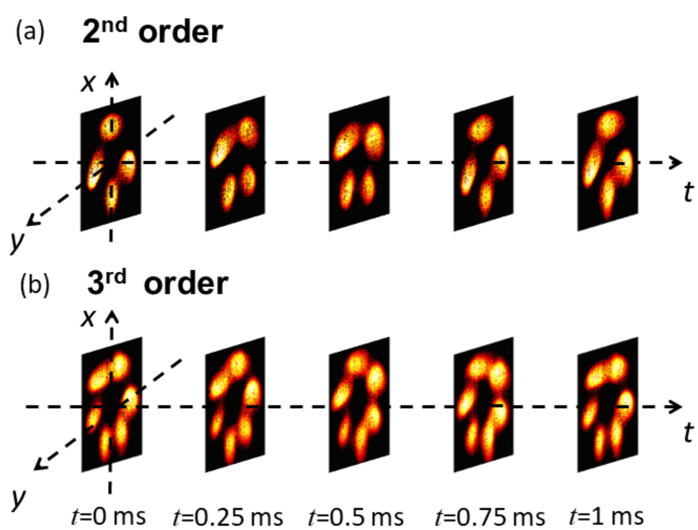

Fig. 6. (a) and (b) show polarization rotation of 2nd and 3rd CVBs at every 0.25 ms when the heterodyne frequency is set to 1 kHz.

5. Conclusion

In summary, we experimentally demonstrated a versatile method to generate femtosecond CVBs with controllable rotated polarization structures. By modulating the frequency domain of two optical vortices with opposite topological charges, time varying polarization of CVBs can be obtained. The results reveal that the high-speed polarization rotation ranging from 1 kHz to 1 MHz can be successfully controlled via changing heterodyne frequency. What's more, the presented approach enables the rotation of higher order CVBs with more complex polarization patterns. The generated CVBs is a type of ultrashort pulse laser, thus offering the opportunity for more classical and quantum applications based on nonlinear effects. Going forward, we anticipate that such a simple yet extremely flexible and powerful way of generating femtosecond CVBs with controllable polarization rotation will stimulate further research into the complex structuring of light, harnessing the polarization degree of freedom of light.

Optics EXPRESS

Funding. National Natural Science Foundation of China (62105237, 61827821, 61975144).

Disclosures. The authors declare no conflicts of interest.

Data availability. Data underlying the results presented in this paper are not publicly available at this time but may be obtained from the authors upon reasonable request.

References

1. Q. Zhan, "Cylindrical vector beams: from mathematical concepts to applications," Adv. Opt. Photonics **1**(1), 1–57 (2009).
2. T. A. Nieminen, N. R. Heckenberg, and H. Rubinsztein-Dunlop, "Forces in optical tweezers with radially and azimuthally polarized trapping beams," Opt. Lett. **33**(2), 122–124 (2008).
3. Q. Zhan, "Trapping metallic rayleigh particles with radial polarization," Opt. Express **12**(15), 3377–3382 (2004).
4. S. Roy, K. Ushakova, Q. V. D. Berg, S. F. Pereira, and H. P. Urbach, "Radially polarized light for detection and nanolocalization of dielectric particles on a planar substrate," Phys. Rev. Lett. **114**(10), 103903 (2015).
5. B. Hafizi, E. Esarey, and P. Sprangle, "Laser-driven acceleration with Bessel beams," Phys. Rev. E **55**(3), 3539–3545 (1997).
6. Z. Rong, C. Kuang, Y. Fang, G. Zhao, Y. Xu, and X. Liu, "Super-resolution microscopy based on fluorescence emission difference of cylindrical vector beams," Opt. Commun. **354**, 71–78 (2015).
7. G. Milione, M. P. J. Lavery, H. Huang, Y. Ren, G. Xie, T. A. Nguyen, E. Karimi, L. Marrucci, D. A. Nolan, R. R. Alfano, and A. E. Willner, "4 × 20 Gbit/s mode division multiplexing over free space using vector modes and a q-plate mode (de)multiplexer," Opt. Lett. **40**(9), 1980–1983 (2015).
8. G. Milione, T. A. Nguyen, J. Leach, D. A. Nolan, and R. R. Alfano, "Using the nonseparability of vector beams to encode information for optical communication," Opt. Lett. **40**(21), 4887–4890 (2015).
9. Y. Zhao and J. Wang, "High-base vector beam encoding/decoding for visible-light communications," Opt. Lett. **40**(21), 4843–4846 (2015).
10. X. Weng, L. Du, A. Yang, C. Min, and X. Yuan, "Generating arbitrary order cylindrical vector beams with inherent transform mechanism," IEEE Photonics J. **9**(1), 1–8 (2017).
11. G. Machavariani, Y. Lumer, I. Moshe, A. Meir, and S. Jackel, "Efficient extracavity generation of radially and azimuthally polarized beams," Opt. Lett. **32**(11), 1468–1470 (2007).
12. Z. Bomzon, G. Biener, V. Kleiner, and E. Hasman, "Radially and azimuthally polarized beams generated by space-variant dielectric subwavelength gratings," Opt. Lett. **27**(5), 285–287 (2002).
13. J.-F. Bisson, Y. Senatsky, and K.-I. Ueda, "Generation of Laguerre–Gaussian modes in Nd:YAG laser using diffractive optical pumping," Laser Phys. Lett. **2**(7), 327–333 (2005).
14. Y. Zhao, J. Fan, H. Shi, Y. Li, Y. Song, and M. Hu, "Intracavity cylindrical vector beam generation from all-PM Er-doped mode-locked fiber laser," Opt. Express **27**(6), 8808–8818 (2019).
15. R. Ismaeel, T. Lee, B. Oduro, Y. Jung, and G. Brambilla, "All-fiber fused directional coupler for highly efficient spatial mode conversion," Opt. Express **22**(10), 11610–11619 (2014).
16. H. Liu, H. Li, Y. Zheng, and X. Chen, "Nonlinear frequency conversion and manipulation of vector beams," Opt. Lett. **43**(24), 5981–5984 (2018).
17. J. Zhao, J. Fan, R. Liao, N. Xiao, and M. Hu, "High-power femtosecond cylindrical vector beam optical parametric oscillator," Opt. Express **27**(23), 33080–33089 (2019).
18. Y. Jiang, T. Narushima, and H. Okamoto, "Nonlinear optical effects in trapping nanoparticles with femtosecond pulses," Nat. Phys. **6**(12), 1005–1009 (2010).
19. L. Paterson, M. P. MacDonald, J. Arlt, W. Sibbett, P. E. Bryant, and K. Dholakia, "Controlled rotation of optically trapped microscopic particles," Science **292**(5518), 912–914 (2001).
20. A. L. Porta and M. D. Wang, "Optical torque wrench: Angular trapping, rotation, and torque detection of quartz microparticles," Phys. Rev. Lett. **92**(19), 190801 (2004).
21. S. Datta and B. Das, "Electronic analog of the electro-optic modulator," Appl. Phys. Lett. **56**(7), 665–667 (1990).
22. J. C. Cheng, L. A. Nafie, S. D. Allen, and A. I. Braunstein, "Photoelastic modulator for the 0.55–13-µ;m range," Appl. Opt. **15**(8), 1960–1965 (1976).
23. W. Liu, D. S. Dong, H. Yang, Q. H. Gong, and K. B. Shi, "Robust and high-speed rotation control in optical tweezers by using polarization synthesis based on heterodyne interference," Opto-Electron. Adv. **3**(8), 200022 (2020).
24. Y. Q. Zhang, J. F. Shen, C. J. Min, Y. F. Jin, Y. Q. Jiang, J. Liu, S. W. Zhu, Y. L. Sheng, A. V. Zayats, and X. C. Yuan, "Nonlinearity-Induced Multiplexed Optical Trapping and Manipulation with Femtosecond Vector Beams," Nano Lett. **18**(9), 5538–5543 (2018).
25. M. Müller, A. Klenke, A. Steinkopff, H. Stark, A. Tünnermann, and J. Limpert, "3.5 kW coherently combined ultrafast fiber laser," Opt. Lett. **43**(24), 6037–6040 (2018).
26. L. Kopf, J. R. D. Ruano, M. Hiekkamäki, T. Stolt, M. J. Huttunen, F. Bouchard, and R. Fickler, "Spectral vector beams for high-speed spectroscopic measurements," Optica **8**(6), 930–935 (2021).
27. S. Matsuo, "Matrix calculus for axially symmetric polarized beam," Opt. Express **19**(13), 12815–12824 (2011).
28. K. J. Moh, X. C. Yuan, J. Bu, D. K. Y. Low, and R. E. Burge, "Direct noninterference cylindrical vector beam generation applied in the femtosecond regime," Appl. Phys. Lett. **89**(25), 251114 (2006).

Optics EXPRESS

29. L. P. Feng, Y. Li, S. H. Wu, X. Guan, C. Yang, W. J. Tong, W. Li, J. F. Qiu, X. B. Hong, Y. Zuo, H. X. Guo, E. H. Chen, and J. Wu, "All-fiber generation of arbitrary cylindrical vector beams on the first-order Poincare sphere," Photonics Res. **8**(8), 1268–1277 (2020).
30. A. Asahara, S. Shoji, and K. Minoshima, "Optical combs and optical vortices combined for spatiotemporal manipulation of light and matter," arXiv:2005.04705 (2020).
31. Y. Zhang, X. Dou, Y. Yang, C. Xie, and J. Bu, "Flexible generation of femtosecond cylindrical vector beams," Chin. Opt. Lett. **15**(3), 030007 (2017).